

## Contents

Summary.....	7
The LaJet LEC-460 Concentrator .....	9
Fluxmapping Device.....	11
The Flux Probe .....	12
The 3-D Scanning Mechanism .....	13
Control and Data Acquisition .....	14
Data Representation and Reduction.....	14
Experimental Setup .....	14
Test Results and Discussion .....	14
Conclusions.....	19
References.....	19

## Figures

1 The LEC-460 Solar Collector .....	10
2 Facet Layout for the LEC-460 .....	11
3 Details of the Drive Area .....	11
4 Mounting Details of the Fluxmapper .....	12
5 Scanning Mechanism of the Fluxmapper .....	13
6 3-D Flux Plot, November 27, 1985 .....	15
7 Isoflux Contour Plot, November 27, 1985 .....	16
8 3-D Flux Plot, February 11, 1986 .....	16
9 Isoflux Contour Plot, February 11, 1986 .....	17

## Tables

1 LEC-460 Facet Groups .....	11
2 Summary of Fluxmap Tests .....	15
3 Normalized Integrated Power Estimates for LEC-460 Flux Measurements .....	17
4 Breakdown of Collector Losses .....	18

DISTRIBUTION: (continued)

California Energy Commission  
Attn: Alec Jenkins  
1516 9th St.

Electric Power Research Institute (2)  
Attn: J. E. Cummings  
E. A. Demeo

## Summary

The optical performance of the LaJet Energy Corporation's membrane-faceted concentrator, Model LEC-460, was evaluated at Sandia National Laboratories' Distributed Receiver Test Facility (DRTF) in Albuquerque during the period from October 1985 through February 1986. This collector model is the same as the units installed at LaJet's Solar Plant I in Warner Springs, California.<sup>1,2</sup> A device that measures flux intensity with a movable Kendall radiometer was used to map the flux distribution at the concentrator's receiver aperture plane, and three-dimensional flux intensity plots and flux contour maps were produced from the data. Numerical integration of the data was performed to obtain an estimate of the total integrated power into the aperture plane.

The fluxmapping of the 43-m<sup>2</sup> collector yielded a measured peak flux of 172 W/cm<sup>2</sup> and an estimated total integrated power of 30.2 kW. These two values are based on normalization of the data with respect to the nominal insolation on a clear day, 0.1 W/cm<sup>2</sup>. Eighty-nine percent of the 30.2 kW was measured within a circle 25.4 cm (10 in.) in diameter around the beam's centroid. The net efficiency of the collector in a clean mirror condition was estimated to be 77.4%. Facet reflectivity and facet soiling were the greatest contributors to collector losses: facet reflectivity was 82.2%, and facet soiling further reduced collector reflectivity by as much as 7.3%.

The results are a conservative performance indicator for the current LEC-460 unit, as the reflective facets on the collector tested received no maintenance or cleaning after installation.

### DISTRIBUTION: (continued)

Georgia Power Co.  
Attn: E. Ney  
7 Solar Circle  
Shenandoah, GA 30264

John Lucas  
865 Canterbury Rd.  
San Marino, CA 91108

Martin Marietta Corp.

## An Evaluation of the LEC-460 Solar Collector

### The LaJet LEC-460 Concentrator

The LEC-460 solar collector has a nominal diameter of 10 m and an average focal length of 5.55 m. Its total collection area is 43.1 m<sup>2</sup> (460 ft<sup>2</sup>, hence 'LEC-460'), of which 41.3 m<sup>2</sup> is estimated by LaJet engineers to be unshaded. Its total weight, not including its foundation, is 1550 kg. Illustrations of the concentrator are provided in Figures 1, 3, and 4.

There are 24 energy-collecting facets per collector; each facet consists of an aluminized, 0.5-mm (2-mil)-thick polyester film membrane stretched over a hoop or shallow drum 1.52 m (5 ft) in diameter. The facet film used is 3M's aluminized ECP-91 film, which has a nominal reflectivity of 0.86. The facet achieves its concave shape by means of a slight vacuum applied through a small tube inserted into the back of the facet.

The facets are supported on a space-frame assembly made of steel tubing 2.5 cm in diameter (28 gauge, 1 in.) (see Figure 1). The tetrahedral frame, which suspends the space frame from the diurnal beam, is made of tubes 0.32 cm (0.125 in.) thick and 8.9 cm (3.5 in.) in diameter. The concentrator's receiver mounting ring is supported above the collector facets by a tripod attached to the base of the tetrahedral frame. The receiver, the receiver mounting ring, and their supporting tripod serve as a counterweight to the facets and the space frame in order to balance the moment of the concentrator about the diurnal drive. Because the LEC-460 was assembled at the DRTF without a receiver, substitute counterweights in the form of steel

rings were bolted to the back of the receiver ring. The pedestal of the collector is made from welded 7.6×7.6×0.95 cm (3×3×0.375 in.) channel.

The distance from a given facet surface to the receiver increases as one moves from the center to the outside edge of the space frame; the desirable facet focal length increases accordingly. Six facet groups are selected according to focal length, the shortest length being 5.35 m, the longest 5.70 m (Figure 2). Table 1 summarizes the information about these facet groups; the letter designation for the facets refers to their positions on the concentrator indicated in Figure 2.

The concentrator is equipped with a polar mount with declination and diurnal (hour-angle) drives. The declination drive positions the concentrator to the declination angle appropriate to the current day of the year and makes occasional adjustments to correct for structural misalignments and other errors. Its action is infrequent. The diurnal drive tracks the sun across the sky, maintaining the collector at the correct hour angle.

The diurnal drive is a 3600:1 double-reduction worm powered by a 93-W (1/8-hp), 36-rpm output gear motor. The output gear rotates the 15-cm (6-in.)-dia steel diurnal tube that supports the space frame structure. The declination drive is a 3.2-cm (1.25-in.) Acme screw with a Teflon impregnated, electroless-nickel coating driven by a 1:1 single-reduction worm and powered by a second identical 93-W motor. All bearings are made from composite materials and run on Teflon surfaces. The declination drive has a polymer-based drive nut. Figure 3 illustrates in detail the diurnal and declination drives.

DISTRIBUTION: (continued)

Parsons of California  
Attn: D. R. Biddle  
3437 S. Airport Way  
Stockton, CA 95206

Sanders Associates  
Attn: B. Davis  
MER 15-2350  
C.S. 2035

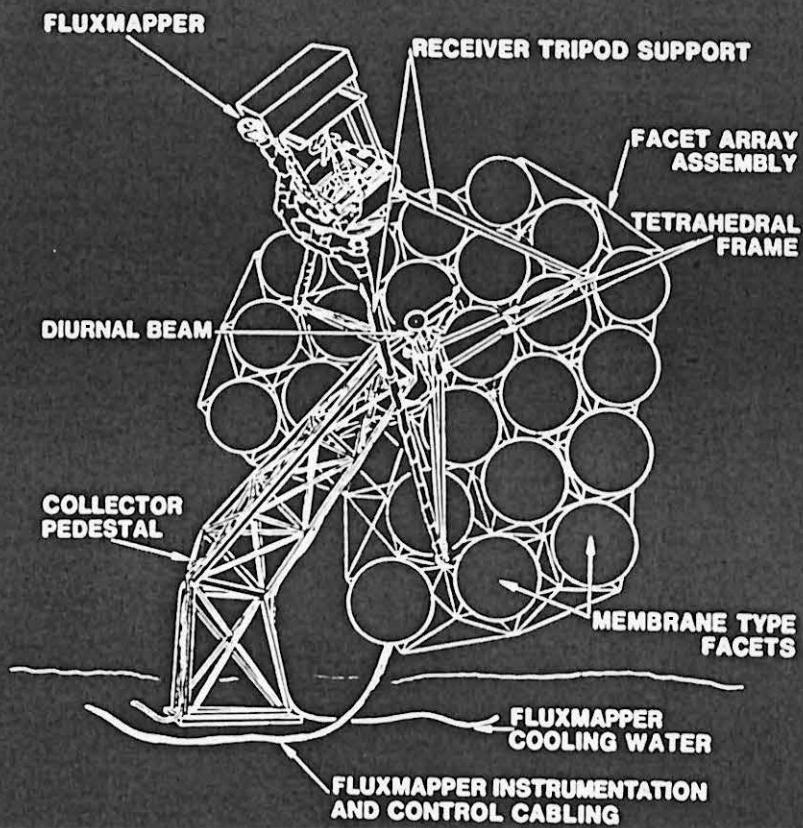


Figure 1. The LEC-460 Solar Collector

DISTRIBUTION: (continued)

SLEMCO  
 Attn: A. J. Slemmons  
 19655 Redberry Dr.

Texas Tech University  
 Dept. of Electrical Engineering  
 Attn: E. A. O'Hair  
 P.O. Box 4489

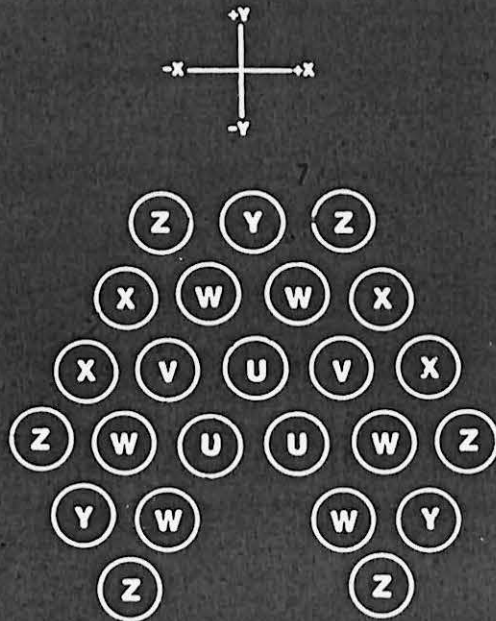


Figure 2. Facet Layout for the LEC-460 Collector

Table 1. LEC-460 Facet Groups

Focal Type Designation	Focal Length		No. of Facets
	(m)	(in.)	
U	5.35	(210.8)	3
V	5.41	(213.0)	2
W	5.47	(215.4)	6
X	5.58	(219.5)	4
Y	5.66	(222.6)	3
Z	5.70	(224.4)	6

The tracking control for the LEC-460 at the test facility is a microprocessor-implemented system consisting of ephemeris tracking with error feedback from four resistance-temperature devices (RTDs) posi-

tioned around the receiver ring. At Solar Plant I, ephemeris data were calculated by a host computer and down-loaded to the local concentrator controllers. At Sandia's DRTF, the Julian date was input to the collector's control processor, and the collector was manually positioned to point at the sun. The processor was placed in automatic-tracking mode and collected tracking data as it followed the sun with the RTD-based analog tracking system. Thereafter, the collector tracked the sun based on the ephemeris data in its memory and the error signals from the RTDs.

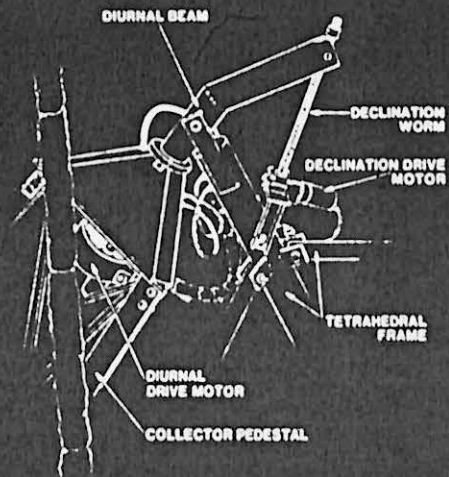


Figure 3. Details of the Drive Area

## Fluxmapping Device

The fluxmapping device used to evaluate the LEC-460 was designed and built for the Solar Thermal Program by engineers at the Jet Propulsion Laboratory, California Institute of Technology.<sup>4</sup> Figure 4 is a sketch of the device shown mounted on the receiver ring of the LEC-460. Its components are described below.

DISTRIBUTION: (continued)

US Robotics  
Attn: Paul Collard  
8100 N. McCormack Blvd.

1824 J. N. Sweet  
1830 M. J. Davis  
1832 W. B. Jones

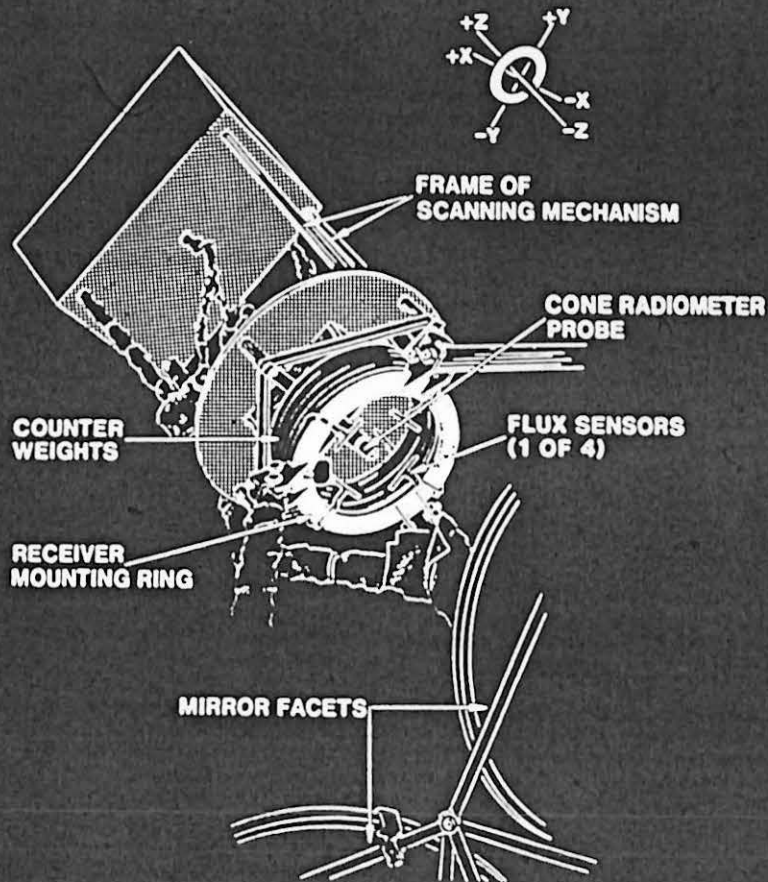


Figure 4. Mounting Details of the Fluxmapper

### The Flux Probe

Flux measurements were made with a Kendall radiometer having a full-scale range of  $1000 \text{ W/cm}^2$  and a resolution equal to 1% of full range. The output of the instrument (up to 10 mV) is obtained from 30 chromium-constantan thermocouples in series measuring the temperature difference between two copper cones, one exposed to the solar radiation, the other shielded and water-cooled. The radiometer has a thermal time constant of  $\sim 0.25 \text{ s}$  and reaches 99.7% of its final value within 8 s. A maximum of 5 s is required to reach a steady state for satisfactory measurement.

Flux measurements can be made in two modes: the cone-absolute mode, in which the absolute value of the incident flux is measured, and the cone-relative mode, in which the measured flux is normalized to the value of the sun's intensity as measured concurrently with a normal incidence pyroheliometer.

Calibration is made by means of a four-wire electric heater built into the probe. The multiplying factor for the calibration, a programmable variable, is adjusted so that the probe's output matches the measured input power to the heater.

### The 3-D Scanning Mechanism

The probe is positioned in the flux field by a scanning mechanism, depicted in Figure 5. The mechanism consists of a square framework supporting a movable carriage upon which the flux sensor is mounted. Stepper motors and a cable system move the flux probe in the flux plane (the xy plane) perpendicular to the concentrator axis (z axis). Flux measure-

ments can be made in a 16×16-in. area in the xy plane; the z-axis drive has a 16-in. range of movement provided by a rack gear and a dc motor.

The scanning mechanism's positioning resolution and speed are 0.01 in. and ~3 in./s, respectively. In operation, a raster is made of the Kendall in equally sized steps across the xy plane, stopping at each measurement point long enough for the Kendall output to settle.

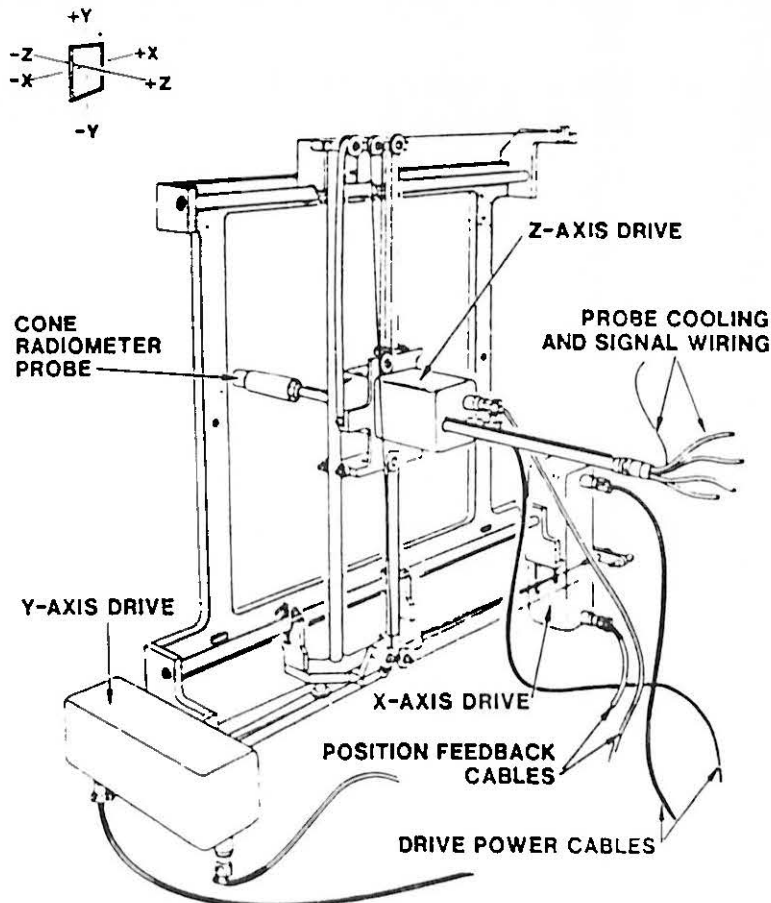


Figure 5. Scanning Mechanism of the Fluxmapper

## Control and Data Acquisition

The fluxmapper's three drive motors are controlled and data are acquired by two preprogrammed microprocessors that communicate by a common random-access memory (RAM). The user accesses the control processor from a CRT terminal via an RS-232 link. Acquired fluxmap data can be "dumped" to an external device, such as a magnetic tape drive or another computer, by means of another RS-232 line. An electronically shielded box located behind the scanning mechanism houses signal conditioning and control electronics.

## Data Representation and Reduction

The fluxmap data from the device's microprocessor are in an ASCII file containing header information, and the time, radiometer position, and flux intensity (in engineering units) for each flux measurement. The test data were transferred to an IBM-XT using the communications program VTERM, and rewritten into a more readable and self-explanatory ASCII file.

Contour maps, 3-D plots, and numerical integration of the data were generated by software developed at Sandia's Flux Gauge Calibration Station where flux measurements are routinely made. To use that software, it was necessary to rewrite the data file into a compatible format. The numerical integration scheme employed performed a summation of the product of the flux intensity and the square area around it (over the entire fluxmap) to obtain an estimate of the total power.

## Experimental Setup

The concentrator facets were installed ~7 months before the first fluxmap tests were performed. Before each facet was installed, its focusing tube was adjusted to obtain the focal length specified. The facets were aligned by the same technique employed by La-Jet at their Warner Springs facility: a facet close to the collector's vertex was manually positioned to reflect its focused energy into the receiver ring while the concentrator tracked the sun; the other facets were kept unfocused (vacuum lines disconnected). The former facet's focal spot served as a reference for adjusting the remaining facets. Each facet was focused and its beam aimed at the referenced focal spot; its fasteners were then tightened to fix it in position. After defocusing the facet, the procedure was repeated on the next facet.

All fluxmap tests were performed at the aperture plane of the LEC-460. The fluxmap device was mounted to the backside of the LEC-460 mounting ring (Figure 1). Water-cooling lines and signal and power cabling were routed down the mounting ring pods and to the ground.

Because the fluxmap device was designed for an azimuth/elevation-driven concentrator, substantial difficulty was experienced operating it on the LEC-460, which has a polar mount. Specifically, the drive motor for the horizontal axis was unable to drive the probe when that axis was tilted  $> \sim 5^\circ$  from horizontal. As a result, all fluxmap tests had to be conducted in a 1-hr time window about solar noon. Because of this and other maintenance difficulties with the fluxmapper, only two satisfactory tests were performed.

## Test Results and Discussion

The results of the two successful fluxmaps—performed November 27, 1985, and February 11, 1986—are reported here. On both dates, steady insolation and clear sky conditions prevailed, and the Kendall probe was operated in the cone-absolute mode. During the fluxmapping, the standard deviation in the insolation measurements was  $< 3\%$ , of average. Subsequently, an average insolation during each test period was used to normalize the data to  $0.1 \text{ W/cm}^2$ . The test parameters and test results are summarized in Table 2. The three-dimensional intensity and isoflux contour plots for the two fluxmap test days are provided in Figures 6 through 9.

The measured peak flux levels were  $169.5$  and  $175.2 \text{ W/cm}^2$  for the two tests. When these measurements are normalized to  $0.1 \text{ W/cm}^2$  they equate to concentration ratios of  $1720$  and  $1704$ , respectively. The two contour plots (Figures 7 and 9) reveal that, although the isoflux contours are not particularly symmetric or smooth, the flux fields are largely contained within small circles, compared to the  $51\text{-cm}$ -dia receiver mounting ring of the LEC-460.

Numerical integration of the flux measurements yielded an estimate of the total normalized power contained within the measured flux field. The estimates obtained for the November 27th and February 11th test dates were  $30.2$  and  $25.2 \text{ kW}$ , respectively. A circle  $25.4 \text{ cm}$  ( $10 \text{ in.}$ ) in diameter about the flux centroid contained  $88.7\%$  of the total power for the November 27th date and  $96.4\%$  for February 11th. Table 3 summarizes these integrated power values.



**Table 2. Summary of Fluxmap Tests**

	Test Date	
	11/27/85	2/11/86
Average insolation (W/cm <sup>2</sup> )	0.0985	0.103
Peak flux measured (W/cm <sup>2</sup> )		
Actual	169.5	175.2
Normalized	172.1	170.4
Normalized total power (kW)	30.2	25.2
Comments	Clear sky, steady insolation on both days	
Flux measurement spacing (in.)	1.00	0.79
Kendall model	ABSOLUTE	ABSOLUTE

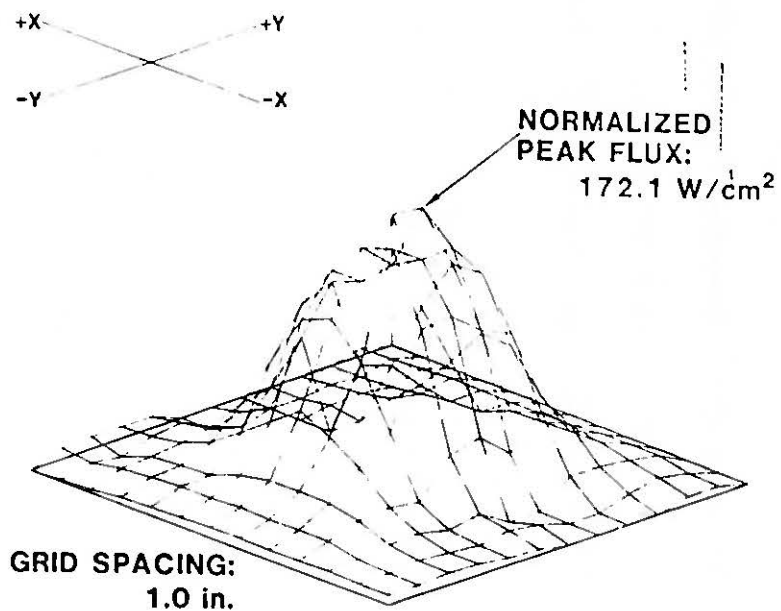


**Figure 6. 3-D Flux Plot, November 27, 1985**

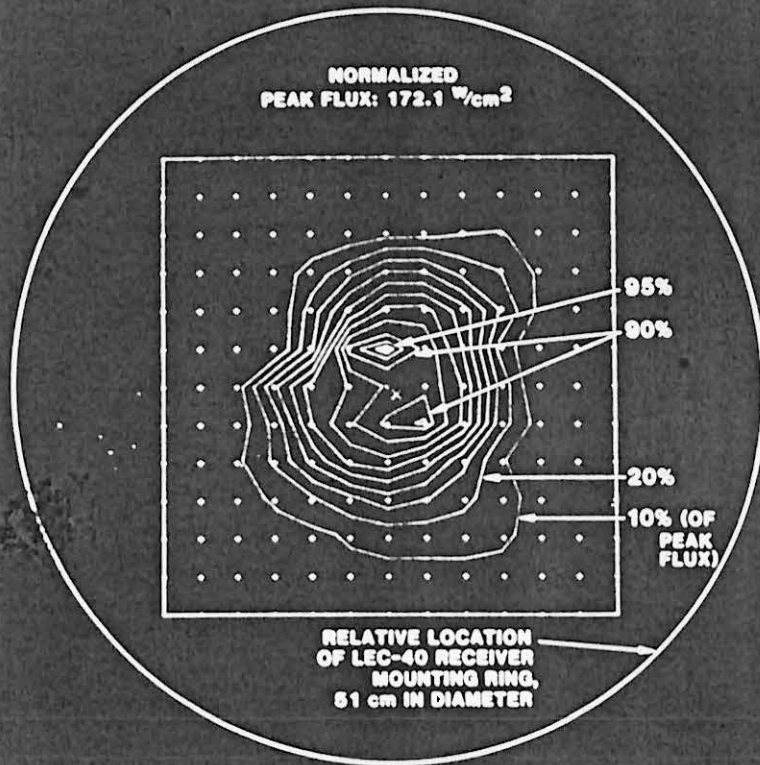


Figure 7. Isoflux Contour Plot, November 27, 1985

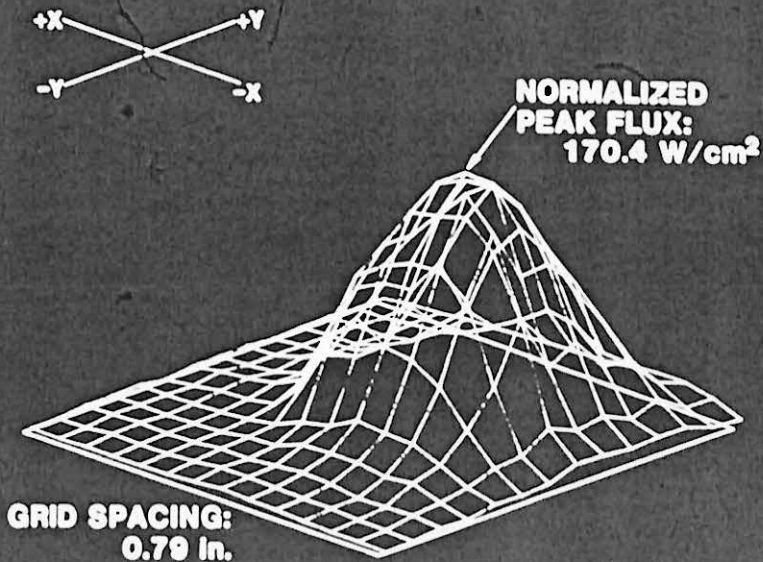


Figure 8. 3-D Flux Plot, February 11, 1986

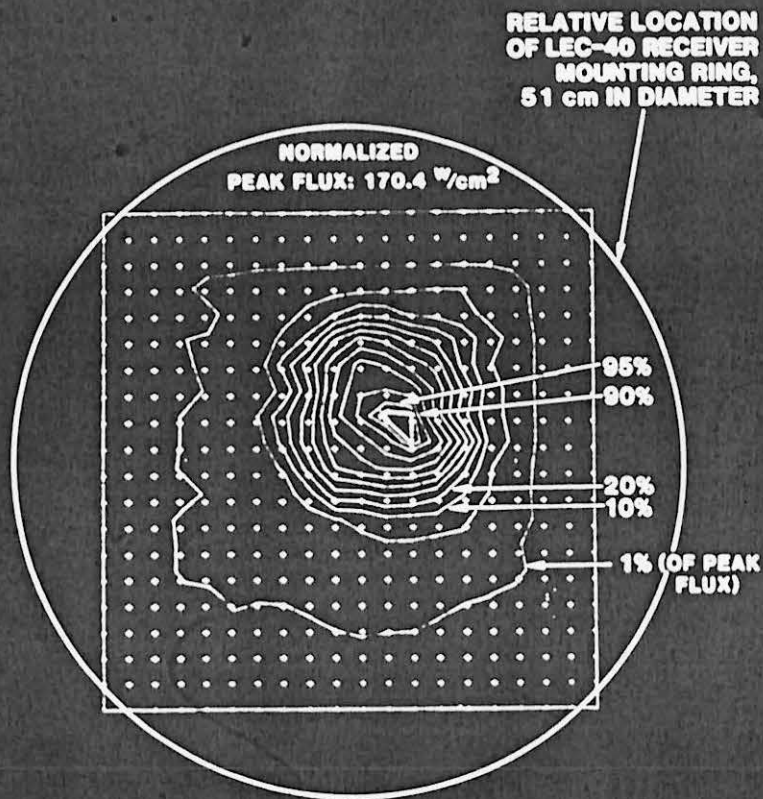


Figure 9. Isopleth Contour Plot, February 11, 1986

**Table 3. Normalized Integrated Power Estimates for LEC-460 Flux Measurements**

Radius of Circle (in.)      (cm)		Estimated Power Within Circle (kW)	
		11/27/85	2/11/86
1	(2.5)	2.9	3.2
2	(5.1)	11.5	11.6
3	(7.6)	19.5	19.1
4	(10.2)	24.5	22.6
5	(12.7)	26.8	24.3
6	(15.2)	28.3	24.9
7	(17.8)	29.7	25.2
8	(20.3)	30.1	25.2
9	(22.9)	30.2	25.2

The total integrated power for the February 11th test (25.2 kW) represents a 17% decline in the performance, compared with the earlier, November 27th test. Possible explanations for this decline include facet misalignment, tracking errors, and reduced facet cleanliness during the February test, and an observed gradual deterioration in the facet hoop-to-facet membrane bond. Details are provided below.

After the November 1985 test but before the February test, it is possible that several facets became misaligned. An evaluation of facet alignment performed in the summer following the fluxmapping indicated that three facets were aimed incorrectly. The power intercepted on a clear day by three facets having 80% reflectivity would be 4.4 kW. This compares closely to the performance difference of 5 kW observed between the two test days.

Another possible explanation is the difference in facet cleanliness on the two test dates. After installation and alignment at the DRTF, they were not cleaned, nor were they given any maintenance in the months prior to the fluxmap tests. The experience at the Test Facility is that the collector facets stored face up tended to become dirtier during brief rains, whereas extended rains could improve the cleanliness of their surface. In July 1986, the summer after the tests were performed, specular reflectivity measurements were made of a facet, first dirty and then cleaned, using the Sandia-developed prototype portable reflectometer.\* The solar-average reflectivity was 74.9% for the dirty facet, and 82.2% for the same facet after cleaning. Thus, the reflectivity of the collector facets may have varied by as much as 7%. The reflectivity measurement has an expected maximum error of  $\pm 2\%$ .

Another contributing factor may have been an offset that existed in the concentrator's tracking during the February 11th test. This tracking offset can be seen from the fluxmap made on that date (Figures 8 and 9). The tracking error was probably due to misalignment of the fluxsensors.

Deterioration in the bond between the polyester film and the metal hoop or ring was observed on some

of the facets in the period following the November test date. On some days during January and February 1986, it was not possible to draw the vacuum on some of the facets because of this debonding. The expected effect of the bond degradation is the defocusing of the given facet and a consequent enlargement of its focal spot. However, integration of the February 11th fluxmap showed the overall flux pattern to be even "tighter" than the November 27th map.

The total normalized power estimate of 30.2 kW for the LEC-460 concentrator represents an overall collector efficiency of 77.4% for the clean mirror condition and 70.1% for the soiled condition. These percentages are based on a measured collection area of 43.1 m<sup>2</sup> and a nominal available solar energy of 0.1 W/cm<sup>2</sup>. A total of 12.9 kW of available energy was lost. Table 4 accounts for contributions to collector losses. The reflectivity and soiling losses account for 80% of the lost power (10.7 of the 12.9 kilowatts).

\*This is a prototype portable reflectometer developed at Sandia, not the Device and Services instrument commonly used there for field measurements. Its wide, flat base permits better positioning on the flexible membrane than would the Device and Services instrument.

**Table 4. Breakdown of Collector Losses**

Measured Power: 30.2 kW

	Power Lost (kW)	Balance (kW)
Power available (starting balance)	—	43.1
Shading (estimated to be 4.2% by LaJet Corp)	1.8	41.3
Reflectivity loss (17.8% of 41.29 kW) (measured)	7.4	33.9
Facet soiling (7.3% of 41.29 kW) (measured)	3.0	30.9
Unaccounted losses	0.7	30.2
<b>Total collector losses: 12.3 kW</b>		
<b>Net collector efficiency (clean condition): 77.4%</b>		
<b>Net collector efficiency (soiled condition): 70.1%</b>		

① SAND 84-2754

## Conclusions

Fluxmap tests of LaJet's LEC-460 concentrator indicate a normalized peak concentration ratio of 1720 ( $172 \text{ W/cm}^2$ ) and a normalized overall power of 30.2 kW. Based on gross reflective area, this represents a collector efficiency of 77.4%, not including the contribution of facet soiling. Eighty-nine percent of the power was contained within a circle 25.4 cm (10 in.) in diameter. The greatest contributors to collector losses were the reflectivity of the facets, which was 82.2%, and facet soiling, which reduced reflectivity by 7.3%.

Maintenance difficulties with the fluxmapper, and the inability to operate the device except during solar noon, prevented the successful completion of more fluxmaps.

The fact that the facets tested on the LaJet concentrator were not given any special maintenance indicates that these results give less than optimal performance values for the LEC-460 unit.

## References

<sup>1</sup>M. McGlaun, "Solar Plant I," *Proceedings of the Distributed Receiver Solar Thermal Technology Conference, Albuquerque, New Mexico, April 1985.*

<sup>2</sup>D. D. Halbert, "Solar Plant I, Design and Performance of Large Solar Thermal Collector Arrays," *Proceedings of the International Energy Agency Workshop, San Diego, California, June 1984.*

<sup>3</sup>J. Scheffer, "Now—Solar Power Cheaper Than Coal, Oil, Gas," *Popular Science*, 226(2):77, February 1985.

<sup>4</sup>W. A. Owen, "The JPL Fluxmapper," *First DOE Distributed Receiver Semiannual Review, Lubbock, Texas, January 1980.* (This is an abbreviated version of an unreleased report on the JPL fluxmapper also written by W. A. Owen, Jet Propulsion Laboratory, California Institute of Technology, Pasadena, California.)